Regional Sources and Sinks of Atmospheric Particulate Selenium in the United States Based on Seasonality Profiles

Citation: Environ. Sci. Technol. 2023, 57, 19, 7401–7409.

As Published: 10.1021/acs.est.2c08243

Publisher: American Chemical Society (ACS)

Persistent URL: https://hdl.handle.net/1721.1/153450

Version: Author's final manuscript: final author's manuscript post peer review, without publisher's formatting or copy editing

Regional sources and sinks of atmospheric particulate selenium in the United States based on seasonality profiles

Isabelle Renee Lao,[†] Aryeh Feinberg,[‡] and Nadine Borduas-Dedekind[*,†]

†*Department of Chemistry, University of British Columbia, Vancouver, Canada*

‡*Institute for Data, Systems, and Society, Massachusetts Institute of Technology, Cambridge, USA*

E-mail: borduas@chem.ubc.ca

Abstract

Selenium (Se) is an essential nutrient for humans and enters our food chain through bioavailable Se in soil. Atmospheric deposition is a major source of Se to soils, driving the need to investigate the sources and sinks of atmospheric Se. Here, we used over 20 years (from 1988 to 2010) of Se concentrations from $PM_{2.5}$ data at 82 sites from the Interagency Monitoring of Protected Visual Environments (IMPROVE) network in the US to identify the sources and sinks of particulate Se. We identified 6 distinct seasonal profiles of atmospheric Se, grouped by geographical location: West, Southwest, Midwest, Southeast, Northeast, and North Northeast. Coal combustion is the most important Se source, with a terrestrial source dominating in the west. We also found evidence for gas-to-particle partitioning in the wintertime in the Northeast. Wet deposition is an important sink of particulate Se, as determined by $Se/PM_{2.5}$ ratios. The Se concentrations from the IMPROVE network compare well to modeled output from a global chemistry-climate model, SOCOL-AER, except in the Southeast US. Our analysis constrains the sources and sinks of atmospheric Se, thereby improving the predictions of Se distribution under climate change.

Keywords: selenium, biogeochemical cycle, $PM_{2.5}$, measurement-model intercomparison, IMPROVE network, seasonality, sources, sinks

Synopsis: There are 6 regions in the US with distinct seasonal profiles of particulate-bound selenium and are driven by anthropogenic and terrestrial emissions as well as wet deposition.

Introduction

Selenium (Se) is an essential dietary nutrient. Its biogeochemical cycle, including its atmospheric component, influences animal and human health through biological processes that regulate our daily lives, like the immune system and thyroid function.[1,2] The recommended dietary intake range of Se is narrow, with safe daily intake levels between 20 to 450 μg for adults.[3] Humans and animals obtain Se from their diet, wherein the Se content of plant-based foods depends on the amount of bioavailable Se in agricultural soils.[4] Precipitation is estimated to account for $35-100*10^8$ g Se per year of global Se deposition compared with $17-24*10^8$ g Se per year via dry deposition.[5] Thus, atmospheric deposition is a major source of Se to agricultural soils,[6,7] and atmospheric cycling of Se is a potential driver for soil Se distribution and trends.[8,9]

Understanding the seasonal cycling of atmospheric Se can help produce Se deposition maps for the agricultural sector to better identify areas that may be at risk for Se deficiency. For other atmospheric compounds, observed seasonal cycles have provided useful information about atmospheric sources,[10] sinks,[11] and transport;[12] however, this information has largely not been exploited for Se measurements. Until now, the analysis of the variability of atmospheric Se has focused on individual field sites over a short time period,[13–15] while broader-scale analyses have focused on annual mean time series.[6] Therefore, apart from a study investigating one year of data in the early 1990s,[16] the broader-scale seasonal patterns of atmospheric Se have not been characterized. A more robust understanding of the seasonality of Se can reveal insights into its atmospheric cycle and subsequent impacts on human, animal, and ecosystem health.

Atmospheric Se is thought to have four main sources: anthropogenic, marine biosphere, terrestrial biosphere, and volcanic emissions.[6,17,18] Anthropogenic sources of Se include coal combustion, metal smelting, and biomass burning, which contribute to an estimated 40% of atmospheric Se flux.[6,17] The marine biosphere accounts for around 35% of atmospheric Se emissions, through direct emission by marine phytoplankton and microbial decomposition of dead phytoplankton species.[17,19] Through the terrestrial biosphere, Se enters the atmosphere from bio-volatilization; this source has been estimated to account for roughly 15% of atmospheric Se.[6,17] Lastly, volcanic activity emits Se-containing compounds and was estimated to contribute to 5% of atmospheric Se globally.[17] While anthropogenic emissions have been cited as a significant contributor to atmospheric Se fluxes in the past,[6,17,18] there is growing evidence that the role of biogenic sources of Se is increasing[8,20] due to declining anthropogenic emissions. The decrease of Se-containing anthropogenic emissions is especially prevalent in North America and Europe from recent emission control technologies and reductions in coal power generation.[8] The decline of anthropogenic emissions and resulting potential redistribution of atmospheric Se source contributions, including its effects on a seasonal timescale, drive the need to investigate the seasonality of Se using a long term dataset.

In this study, we use particulate Se time series from 82 stations in the Interagency Monitoring of Protective Visual Environments (IMPROVE) aerosol dataset to investigate the sources and sinks of particulate Se across the continental United States (US) using seasonality profiles. We compare how the station-specific Se time series vary spatially and temporally across the network. We also probe mechanisms that may influence seasonal atmospheric Se variability, namely the role of emission sources, precipitation, and drivers of enrichment and depletion of Se in particulate matter. Lastly, we compare Se concentrations with model outputs from a global chemistry-climate model to identify when and where models adequately and inadequately represent Se seasonal variability.

Methods

IMPROVE Network and dataset

The Interagency Monitoring of Protected Visual Environments (IMPROVE) Network was established in 1985 to record air quality observations for monitoring conditions in US national parks, national wilderness areas, and national monuments, termed Class 1 areas under the federal Clean Air Act.[21,22] Using the Federal Land Manager Environmental Database, we extracted Se and gravimetric fine mass ($PM_{2.5}$) concentrations, uncertainties, and minimum detection limit values for 229 sites, of which approximately 160 sites are currently active. From the inauguration of the IMPROVE network to January 2011, elements with atomic weights from iron to lead, including Se, were measured using Energy Dispersive X-ray Fluorescence (ED-XRF). Though the XRF data does not provide us with speciation information, it is most likely that the Se analyzed is oxidized Se(IV) or Se(VI).[23] In addition, since the IMPROVE methodology is not optimized specifically for Se, there is a possibility of volatile Se evaporating during storage or sample work-up, implying that the reported Se concentrations are likely lower bonds. For further details on filter sampling conditions at IMPROVE sites, see SI Section 1. Due to an instrumentation change in 2011 and a re-analysis of filters identifying biases in trace metal analyses post 2010,[24] we only used IMPROVE data prior to 2011 (Figure S1-2). Consequently, we used particulate Se time series from 82 stations with at least ten years of Se data pre-2011.

Seasonal profiles for each station were generated by averaging concentrations (in ng m^{-3}) for each day of the year. Then, a monthly moving mean function was applied on the averaged concentrations to obtain an overall seasonal profile for each site (Figures 2). A step-wise graphic and explanation of the procedure to obtain representative seasonal profiles for each station, including effects of different moving mean time windows, can be found in SI Section 1 (Figure S3) and in the SI Binning Document.

Analysis of seasonal profiles

Manual inspection of the 82 Se seasonal profiles revealed a set of similar regional profiles (Figure 2). To quantify this similarity, we used unsupervised clustering algorithms, including principal component analysis, k-means clustering, hierarchical clustering, and a decision tree. The detailed methodology, including the thresholds used for the decision tree and outcomes of the binning analysis for each method, are detailed in the SI Binning Document. The quantitative binning analysis outcomes were used to further inform the manual binning. Overall, sites were first sorted by eye, then the confidence of this sorting was confirmed by unsupervised quantitative methods and the decision tree.

Precipitation and coal power plant emission datasets

To further corroborate and probe sources and sinks influencing the observed Se seasonality, we used a precipitation dataset from the National Oceanic and Atmospheric Administration (NOAA)[25] and coal power plant emission fluxes from a global catalogue of large SO_2 sources derived using the Ozone Monitoring Instrument.[26] Additional details of these datasets are available in SI Section 1.

Global Aerosol-Chemistry-Climate Model Data

We also used simulated data from the aerosol-chemistry-climate model, SOCOL-AER, which includes a comprehensive atmospheric Se scheme[6,23] to further constrain Se sources over the US. We used previously published source-resolved simulations of daily particulate Se concentrations modeled from 1970 to 2017 at 2.8° × 2.8° resolution from Feinberg et al.[6]. While the model does not track chemical speciation for particulate Se, SOCOL-AER does track the transport, transformation, and deposition of Se in 7 gas phase species (H_2Se, DMSe, OCSe, CSe_2, CSSe, oxidized organic Se, and oxidized inorganic Se) and 40 particulate size-bins, covering dry radius sizes from 0.39 nm to 3.2 µm. Details on the rate constants of Se compound gas-phase reactions are included in Table S1. The global Se budget in the SOCOL-AER simulations was 39% marine biogenic emissions, 34% anthropogenic emissions, 15% terrestrial biogenic emissions, and 12% volcanic emissions, for a total of 32 Gg Se yr^{-1}.[6] These values were derived from a compiled dataset of atmospheric Se observations using Bayesian inversion, a method to calibrate model parameters from available observations.[6]

The spatial and temporal distribution of anthropogenic, volcanic, and marine biogenic sources were assumed to follow sulfur emission inventories, since Se and sulfur compounds are known to have similar physio-chemical properties and correlate in time and space.[17,19,27] Anthropogenic emissions were distributed according to sulfur dioxide emissions from the Community Emissions Data Systems CMIP6 inventory.[28] Marine dimethyl selenide (DMSe) concentrations were scaled from a climatology of dimethyl sulfide (DMS) concentrations,[29] and DMSe emissions were calculated according to an online wind-driven parameterization.[30] Volcanic Se emissions were mapped by scaling sulfur dioxide emissions from the Global Emissions Initiative inventory (GEIA),[31,32] though volcanic activity was not relevant on the seasonal timescale in the continental US. Emissions of volatile Se from the terrestrial biosphere were assumed to follow the mean spatial distribution of volatile organic compound (VOC) emissions from the Model of Emissions of Gases and Aerosols from the Nature-Monitoring Atmospheric Composition and Climate (MEGAN-MACC) inventory.[33] In terms of seasonality, the anthropogenic and volcanic emissions were constant over the year, whereas marine and terrestrial biogenic emissions varied seasonally according to the base inventories. In Feinberg et al.[6], the model was evaluated against annual mean particulate Se observations from the IMPROVE network, showing good model agreement with IMPROVE measurements ($R^2 = 0.66$) and simulated values agreeing within a factor of 2 of measurements at 86% of the IMPROVE sites. A more detailed explanation of the design of the atmospheric Se model and associated uncertainties can be found in Feinberg et al.[6],[23]. In this study, we used the SOCAL-AER model output data to resolve the seasonality of the Se sources and sinks.

Results and discussion

Seasonality of Se

Average annual Se concentrations ranged from 0.10 to 2.10 ng/m^3 from 1988 to 2010 at the IMPROVE measurement sites (Figure 1). The IMPROVE average Se concentrations fall in the range of previous field campaigns in the US, such as a 2-year study in Atlanta, Georgia which recorded an annual mean concentration of 1 ng/m^3[34] and a 15-month study in Queens, New York which recorded an annual mean concentration of 1.1 ng/m^3.[35] These values represented a fraction from 0.0202 to 0.0031 % of the PM$_{2.5}$ mass concentrations (Figure 3).

To identify sources and sinks of particulate Se, we generated seasonal profiles of Se concentration at 82 IMPROVE sites with greater than 10 years of Se data prior to 2011 (see methods for selection criteria). IMPROVE sites are generally located in national parks and wilderness areas, thereby allowing the seasonality analysis to be regionally representative by minimizing the influence of point sources of Se. We find that particulate Se seasonality trends are clearly regional and can be grouped into six distinct profiles: West, Southwest, Midwest, Southeast, Northeast, North Northeast, and one unclassified bin (Figure 2). Unsupervised clustering algorithms, including principal component analysis and k-means clustering, as well as decision trees yielded similar results (see the SI Binning Document for detailed binning analysis parameters and outcomes). The Se seasonal profiles are remarkably different from one another with distinct yet different peaks and troughs occurring throughout the year (Figure 2). These profiles demonstrate that sources and sinks of Se in the US are regional, with important implications for the atmospheric lifetime and transport of Se species.

Seasonality of Se/PM$_{2.5}$ ratios

Next, we investigated whether PM$_{2.5}$ concentrations had coinciding seasonal peaks and troughs as the Se concentrations to identify similarities between sources and sinks. Using the same seasonality-derived regional classification as in Figure 2, we found that $PM_{2.5}$ grouped in the same regions are similar, but clearly distinct and in some cases opposite to Se seasonality (Figure 2 & S4, blue traces). This observation led us to calculate $Se/PM_{2.5}$ ratios at each site to identify seasons of Se-enrichment and Se-depletion in $PM_{2.5}$. Se-enrichment occurs when the $Se/PM_{2.5}$ ratio is above the bin mean and is particularly prevalent in the wintertime (Figure 3). Conversely, Se-depletion occurs when the $Se/PM_{2.5}$ ratio is below the bin mean and is evident in the summertime (Figure 3). These distinct regimes highlight that the seasonality in Figure 2 is unique to Se and can be used to identify sources and sinks of particulate Se in the US.

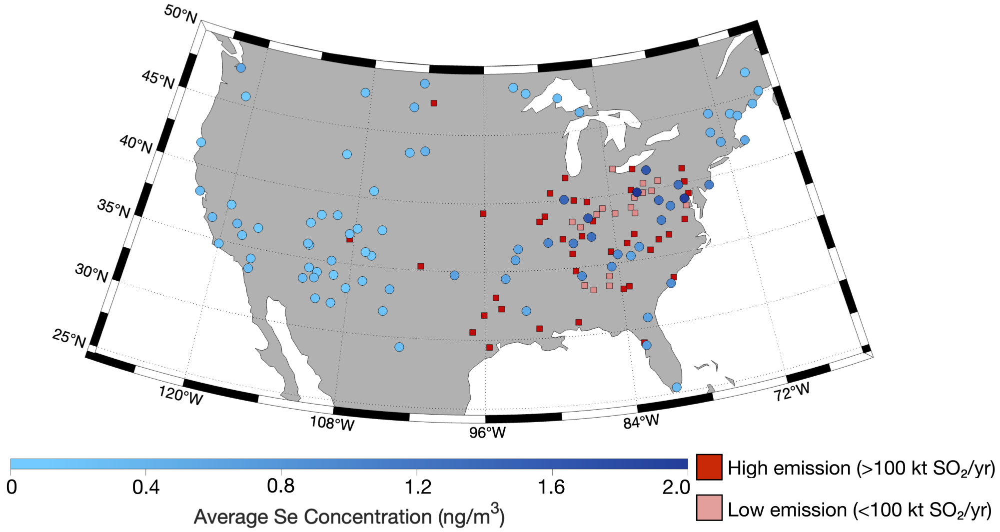

Figure 1: Circular scatter points on map represent 82 IMPROVE sites with more than 10 years of Se data pre-2011 colored by their average annual concentration of particulate Se from 1988 to 2010. Average annual power plant emission flux from global catalogue[26] between 2005 to 2010 represented by colored squares, where pink and red represent low and high emission flux, respectively.

Impact of coal emissions (Northeast and North Northeast)

The stations assigned to the Northeast bin have the highest average Se concentration of all the IMPROVE network sites (Figure 3b & 1). They are characterized by peak Se concentrations in the summer and winter, and troughs in the spring and fall (Figure 2, red trace). The

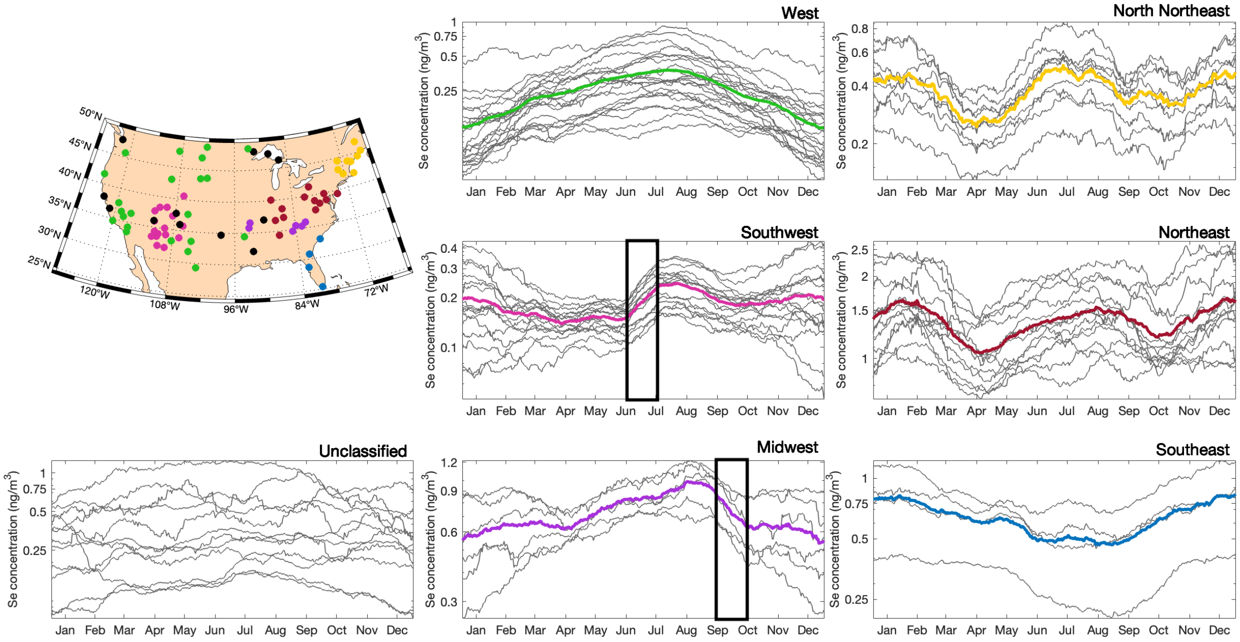

Figure 2: Seasonal profiles of particulate Se concentration time series from the IMPROVE network show that regionally similar stations have similar profiles. Stations are grouped based on their seasonal profile. Colored average value of all seasonal profiles correspond to station location marker on map from 1988 to 2010. Black boxes in time series highlight characteristic periods of the given seasonal profile trace.

highest average concentration over the analysis period was observed at a station located in Quaker City, Ohio at 2.10 ng/m^3. The highest Se measurement recorded during this period was 28.61 ng/m^3 on February 24, 2009 at M. K. Goddard State Park in Pennsylvania within the Northeast bin. Furthermore, stations in the North Northeast bin experience the same seasonality. However, Se concentrations at these stations are a factor of 10 lower, consistent with these stations being located downwind of the Northeast stations where the coal power stations are located (Figure 2, yellow trace). More broadly, average Se concentrations are greater in the eastern US than the western US (Figure 1). This finding is consistent with Eldred et al. who found that Se concentrations in the Appalachian mountains were ten times higher than in the Pacific Northwest.[16]

Emissions from coal power plants are a known source of atmospheric Se.[18,36] We investigated the hypothesis that sites with high atmospheric Se concentrations were located in regions with high coal emissions by plotting power plant location and emission flux mag-

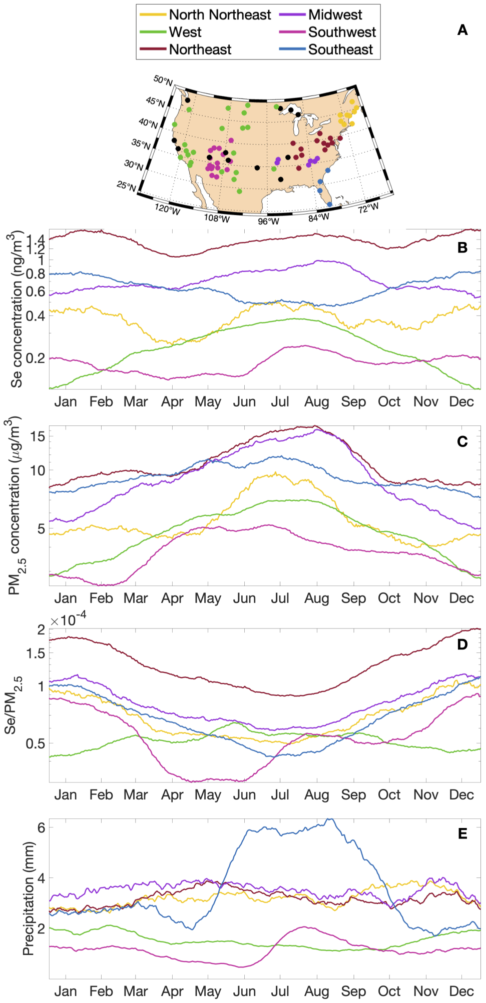

Figure 3: From top to bottom: a) station location, b) Se concentration, c) fine mass concentration, d) Se/PM$_{2.5}$ fraction, e) precipitation, of each Se concentration seasonal profile identified. Colored mean value of all seasonal profiles correspond to station location marker on map. Precipitation figure is based on NOAA reanalysis data.

nitude with average Se concentrations from the IMPROVE network (Figure 1). Sites in the Northeast bin measure greater than 1.35 ng m^{-3} Se on average, whereas the overall US average is 0.50 ng m^{-3}. This correlation emphasizes coal emissions as an important source of Se to the atmosphere.

In addition, we observe distinct Se-enrichment in $PM_{2.5}$ in the wintertime due to an increase in Se concentration in the Northeast and North Northeast. We hypothesize that this wintertime enrichment is linked to coal combustion in the Northeast and the North Northeast and is potentially due to local meteorology and/or gas phase chemistry. The enrichment can not be attributed to increased $PM_{2.5}$ in the winter, because $PM_{2.5}$ concentrations decrease in the wintertime at all sites (Figure 3c). It is likely that meteorology plays a role, as the model which assumes seasonally invariant anthropogenic emissions, reproduces the increase in Se during winter (see section on model comparison and Figure 5b-c). Coal emissions remain relatively constant over the year, so it is possible that gas phase Se in the Northeast and the North Northeast of the US is condensing into existing particles during the cold wintertime, thereby enriching Se in $PM_{2.5}$.[37] There is evidence that approximately a third of Se is vaporised in a coal-fired steam plant.[38] In fact, Ondov et al. observed that particulate Se was enriched by a factor of 6 in a dispersing plume of a coal-fired power plant compared to Se in the stack.[39] Similarly, Tuncel et al. observed increasing partitioning of Se to particulate matter as coal power plant plumes age.[40] While the chemical characteristics and mechanistic behaviour of gas-phase Se requires both more laboratory experiments and field measurements to further constrain, this unique wintertime increase in Se concentrations in $PM_{2.5}$ is evidence of the presence of gas phase Se in our atmosphere as a source for Se in $PM_{2.5}$.

Precipitation anti-correlated to Se concentrations (Southeast)

Similar to $PM_{2.5}$, particulate Se's main removal mechanism is wet deposition, accounting for around 80% of all Se deposition.[5,6,17,37] We hypothesized that periods of higher precipitation lead to lower Se and $PM_{2.5}$ concentrations. We used precipitation reanalysis data available through NOAA and determined the mean precipitation seasonality at each bin (Figure 3e). Next, we determined the correlation between particulate Se concentrations and precipitation (Figure 4). As expected, Se is anti-correlated with precipitation in some regions, namely the Northeast, North Northeast, and Midwest bins but the anti-correlation is most apparent in the Southeast bin (Figure 4). Indeed, Se profiles in the Southeast have a unique trough in the summer linked to summertime precipitation between June and September (Figure 2, blue trace). Despite the increased summertime rain in the Southeast, $PM_{2.5}$ concentrations remain high in the summer in the Southeast (Figure 3c & S4). This opposite seasonal trend between Se and $PM_{2.5}$ suggests a summertime source of $PM_{2.5}$ which is low in Se (Figure 3b-d).

In addition to wet deposition, particulate Se can also be removed from the atmosphere through dry deposition. An observational study in Northern China found that the contribution of dry deposition to the total Se sink varied over their 10 measurement sites.[41] It was determined that particle size is an important factor for atmospheric removal of Se, with larger particles being removed faster by dry deposition.[41,42] Prior observational studies have shown that Se is concentrated in the fine aerosol fraction.[37,43,44] The IMPROVE network monitors fine particulate mass, so dry deposition is likely to play a minor role on Se seasonality in this study. Moreover, an analysis of the fraction of Se $PM_{2.5}$ removed by wet deposition in the SOCOL-AER model simulations show that the median wet deposition contribution to total aerosol Se deposition is 88% (84%–91%, 25th–75th percentiles, Figure S6).

Precipitation correlated to Se concentrations (Southwest)

Surprisingly, we observed a positive correlation between Se concentrations and precipitation for stations assigned to the Southwest group and in the northern Great Plains area (Figure 4). Previous field measurements have linked continental moisture sources with terrestrial biogenic emissions of Se.[45] Thus, we hypothesized that a mechanism releasing Se from soil during rain events may be driving this correlation in the Southwest. It is possible that aerosol

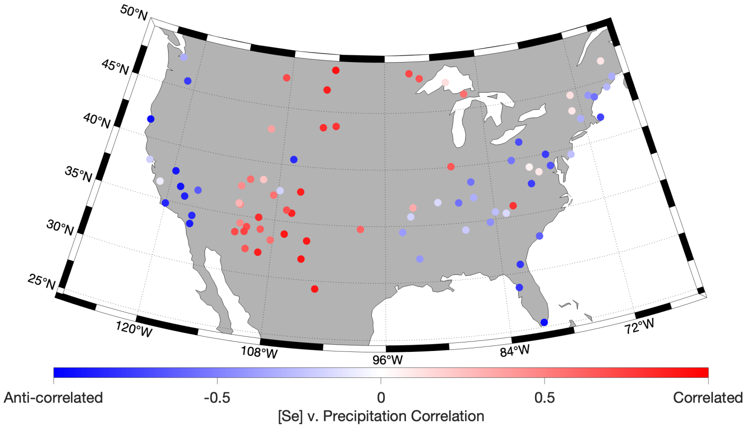

Figure 4: Spearman correlation between seasonal profile of Se at each station and reanalyzed precipitation at nearest grid point from NOAA.

generation is occurring by raindrop impact on soil containing higher concentrations of Se.[46] To explore this mechanism, Se soil concentration maps from the United States Geological Survey were obtained (Figure S7). The northern Great Plains area is an area of particularly high Se concentrations in the US (Figure S7), due to the presence of black shale bedrock.[47] However, in the Southwest region, where particulate Se concentrations and precipitation were also correlated, Se soil concentrations are not anomalously high compared to the rest of the country (Figure S7). Therefore, although high Se soil concentrations can help explain the correlation between precipitation and atmospheric Se concentration in the northern Great Plains, it cannot explain the precipitation-induced Se source in the Southwest.

Of note, the Southwest seasonal profiles are characterized by a rapid increase of Se concentration in June, highlighted by the black box (Figure 2, pink trace). There is a unique and rapid change from Se-depletion to constant Se/PM$_{2.5}$ ratio in the later summer and early fall in the Southwest (Figure 3d). This change coincides with a short period of Se increase in the region during July and August (Figure 2), concurrent with a decrease in PM$_{2.5}$ mass and remarkably increased precipitation (Figure 3). This observation represents compelling evidence that there exists a precipitation-induced source of Se in PM$_{2.5}$, but not of fine particulate mass, leading to a clear Se-enrichment in July and August in the Southwest. Nonetheless, our analysis cannot discriminate whether this source is emitting Se as bioaerosols[48] or as gas phase species which then condense and/or partition to the particle phase.

Additionally, soil properties may still play a role, as the Southwest is a desertous region where dust resuspension of particulate matter containing Se may be occurring. Another potential mechanism is the influence of the biological ecosystem.[46] Volatile Se may be released by the vegetation during precipitation events; for example, precipitation in the Southwest has been found to enhance volatile mercury emissions from soil through displacement of soil gas.[49,50] Additionally, the release of nitrous oxide from soils via aerosolization following a rain event is a known mechanism, especially in arid climates similar to the Southwest.[51] Storage and subsequent release of Se can vary greatly between different soil types and vegetation ecosystems,[52] thereby warranting further research. Understanding what drives the relationship between precipitation and elevated Se concentrations can inform agricultural and health policies in predicting when and where Se oversupply and depletion could occur.

Se tracking $PM_{2.5}$ (West, Midwest)

All stations within the West bin have a characteristic Se concentration peak in the summer, with average concentrations less than 1 ng/m^3 (Figure 2, green trace). Both Se and fine mass concentration profiles have similar shapes in the West bin, suggesting that Se tracks $PM_{2.5}$ (Figure 3b-c, green trace). Consequently, the Se/$PM_{2.5}$ ratio remains relatively constant, and there is little to no Se-enrichment or depletion observed on average (Figure 3d, green trace). In fact, compared to other regions, we observed the smallest range and the lowest average of Se/$PM_{2.5}$ ratio in the West group of profiles (Figure S5 & Table S2). It is worth noting that the West bin also includes the largest geographical spread among all the bins identified, and likely includes multiple mechanisms contributing to the Se/$PM_{2.5}$ ratio.

Furthermore, stations in the Midwest bin were differentiated by a steep decline in Se concentration in September-October as indicated by the black box (Figure 2, violet trace). This decline is concurrent with a decline in $PM_{2.5}$ (Figure 3 & S4), indicative of similar sinks of Se and $PM_{2.5}$. This sink, however, is not precipitation (Figure 3e), yet it is well captured in the model (see measurement-model comparison section), suggesting that meteorology plays a role (Figure 5).

Sites with a constant Se/$PM_{2.5}$ ratio can be interpreted as having similar sources and sinks to the general fate of $PM_{2.5}$ in that region. Major sources of fine particulate matter in the Western US include primary sources, such as soil, biomass burning and industry, and secondary aerosols, such as secondary ammonium nitrate and ammonium sulfate.[53,54] The summertime increase in $PM_{2.5}$ in the West and across the US could be driven by increased biogenic carbon emissions.[55] In addition, summertime photochemistry of both volatile organic carbon and sulfur dioxide can contribute to PM increase.[55] It is possible that photochemistry and oxidation also play a role in Se summertime enrichment by facilitating the conversion to the particulate phase. Oxidation to lower volatility Se species is fast, wherein dimethyl selenide has a measured rate constant with OH radicals of $6.78 \pm 1.70 \times 10^{-11}$ cm^3 $molecule^{-1}$ s^{-1}, providing evidence of fast oxidation reactions of organo-selenium compounds, albeit with unknown product distributions.[23,56] Overall, we can conclude that the sources and sinks of Se are driven by similar mechanisms that influence $PM_{2.5}$ in the West and Midwest.

Se measurement and model comparison

To further understand the impact of emission sources on the seasonal variability of atmospheric Se, we used simulated, source-apportioned Se concentrations from the global atmospheric Se model, SOCOL-AER.[6] We first compared the simulated daily mean Se particulate concentrations to IMPROVE observations, which show good agreement across most of the US (Figure 5, Figure S8). In fact, the median model-measurement correlation over all stations is 0.61 (0.32–0.81, 25th–75th percentiles). Clear exceptions to the model agreement are observed for the Southeastern US and the Great Lakes (Figures S9 & S10). Around the Great Lakes, the site specific Se seasonal profile and SOCOL-AER modeled profile is relatively constant (Figure S9). Furthermore, the Great Lakes region has a positive correlation with precipitation, thereby pointing to unique Se sources related to rainfall, which are not accounted for in the model (Figure S9). In addition, the Southeastern US has clear anti-correlation between the model and IMPROVE observations (Figure 5, Figure S10). We explore what may be contributing to this anti-correlation in a case study of this region in the following section.

The source-apportioned model data provides further insight into the drivers of Se seasonality in the Northeast US. The model accurately simulates the seasonality of observed Se concentrations in the North Northeast, which shows a bimodal seasonal profile with local maxima in summer and winter (Figure 5). The model attributes Se in the North Northeast mainly to anthropogenic sources, corroborating the dominance of coal power plant emissions in this region (Figure 1). Notably, the anthropogenic emissions in the model are seasonally invariant; therefore, the ability of the model to capture North Northeast seasonality points to meteorological factors driving seasonality in this region. In fact, the model is better able to represent Se seasonality from anthropogenic sources alone ($\rho = 0.65$) than with all source contributions ($\rho = 0.50$) in the North Northeast. The model is unable to represent the Northeast group of sites ($\rho = 0.23$) as accurately as the North Northeast stations ($\rho = 0.50$) (Table S3). Since the Northeast group of sites are located closer to anthropogenic emission sources (Figure 1), it may be more difficult for a coarse resolution global model ($2.8^\circ \times 2.8^\circ$) to capture the spatial and temporal variability when close to point sources, compared to downwind North Northeast stations.

Although anthropogenic emissions are the largest source of Se to the atmosphere, terrestrial emissions can also impact Se concentrations. For example, the observations in the West sites have the same correlation with the simulated Se from terrestrial sources alone as with the total simulated Se ($\rho = 0.79$) (Figure 5, Table S3). The observed Se seasonality in the West bin shows a summertime maximum and wintertime minimum, similar to the modelled terrestrial source (although the model shows a narrower peak shifted about a month later). This finding suggests that measurement stations in the West could be used to improve model parametrizations of terrestrial biogenic Se emissions, which are currently scaled to terrestrial VOC emissions.[33] Eldred et al.[16] found better correlations of Se with S in the eastern US than in the western US, suggesting more diverse sources in the West that may not be well captured in existing emission inventories. Our analysis identifies the Western US as a region potentially driven by terrestrial biosphere Se emissions and a region where future field studies would be beneficial to uncover the processes driving terrestrial emissions and their seasonality.

Southeast case study

In the Southeast region, none of the source contributions correlate with observations (Figure 5, Table S3), indicating that the current modelling assumptions are not adequate in capturing the seasonality at these stations. In fact, the model-measurement median ρ for the Southeast is -0.83, whereas the median ρ for all stations excluding he Southeast is 0.62.

The four stations located in the Southeast US have a unique minimum in particulate Se concentrations in the summertime (Figure 2. This summertime trough occurs simultaneously with peak summertime $PM_{2.5}$ and peak precipitation, surpassing rainfall at all other locations (Figure 3e, Figure S10). Noticeably, the SOCOL-AER model and measurement comparison for these Southeast sites are anti-correlated (Figure 5). To investigate whether missing washout in the model was responsible, we compared the modelled precipitation to the observed NOAA reanalysis product and found that SOCOL-AER generally underestimates the precipitation in the Southeast, especially the summertime peaks (Figure S11). This result could be a possible reason for the discrepancy between modelled and measured particulate Se. The underestimation of washout in the Southeast is not a problem unique to SOCOL-AER, as other global models show underestimated mercury wet deposition in the Southeast during the summertime, due to difficulty capturing convective precipitation in coarse resolution models.[57] All sites within this class have similar seasonality profiles of Se concentrations, Se-enrichment, and precipitation profiles, suggesting that the drivers of Se seasonality have a broad regional scale (Figure S10). This observation indicates an unknown, yet unique mechanism governing Se concentrations in this region of the US.

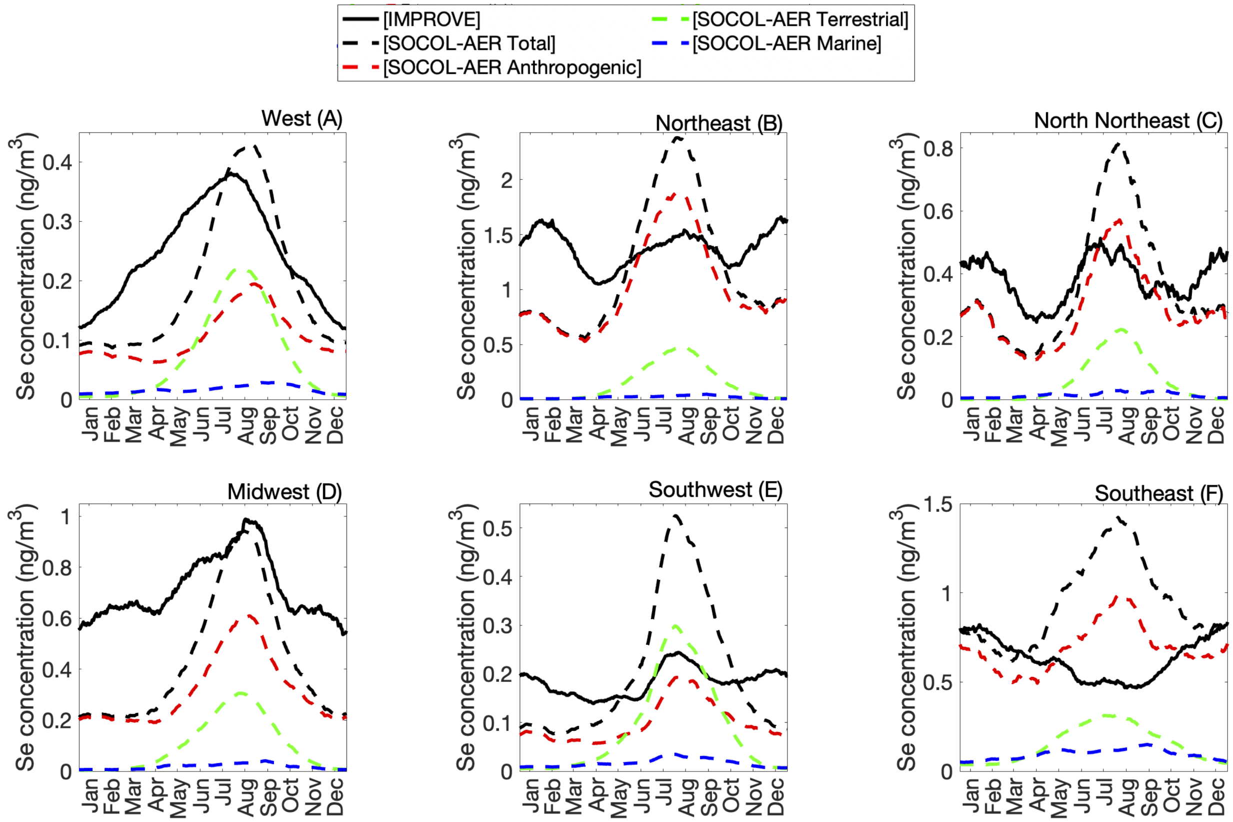

Figure 5: SOCOL-AER simulated source-apportioned Se concentrations and observed Se concentrations from the IMPROVE network based on regional bins. Volcanic source contributions are not shown as they are negligible in the Conterminous US.

Atmospheric Implications

There is clear regionally-dependent seasonal variability of $PM_{2.5}$-bound Se concentrations measured by ED-XRF within the IMPROVE network. Sites with similar seasonal profiles are located in the same geographic region: West, Southwest, Midwest, Southeast, Northeast, and North Northeast (Figure 2). This geographic dependence also implies regional sources and sinks of Se in the atmosphere. We further explored the influence of unique Se emissions sources (Figure 1, 5) and wet deposition (Figure 4) as mechanisms driving the regional seasonality.

In our investigation of wet deposition as a removal mechanism for atmospheric Se, we found that some areas show evidence for precipitation events raining out particulate Se (Northeast, North Northeast, Southeast, and Midwest). Other areas show a distinct enrichment of Se during seasonal precipitation, evidence of released Se by the terrestrial environment during precipitation events in the Southwest and Great Plains area (Figures 4 & S9). It is unknown whether this Se is emitted in the gas phase, particle phase, or both, thereby requiring further investigation. Nonetheless, since soil Se concentration maps could not explain the Se and precipitation correlation in the Southwest, fieldwork would be necessary to further study the mechanism at play and understand Se distribution and variability for informing agricultural practices and policy.

Using the source-apportioned concentration output from the SOCOL-AER global chemistry-climate model, we observed that the driving factors of seasonality of Se are well modelled in some areas (i.e., North Northeast, Northeast, Southwest, Midwest, and West bins), but not others (i.e. Southeast bin) (Figure 5 and Table S3). Anthropogenic emissions datasets, including the CMIP6 SO_2 data used for the Se emissions in the SOCOL-AER model, have annual time resolution and do not include seasonality. Our study provides a baseline for using seasonality to study trends resulting from declining coal emissions across the US (also visible in Figure S1).[8] Biogenic sources of Se are therefore likely to drive Se concentrations in the near future in certain regions of the US. A greater understanding of the relative source contributions to atmospheric Se, including additional modeling studies to quantify the influence of factors like rain and soil, can help the agricultural sector in identifying areas that may be at risk for Se oversupply and deficiency.

This study also serves as a stepping stone in exploring the broader-scale seasonal patterns of atmospheric Se and gives motivation for understanding the chemical composition and formation pathways of atmospheric Se. While current Se lifetimes are constrained based on sulfur parameters,[6] a more robust understanding of the size distribution, products, and speciation of atmospheric Se is necessary to understand the health effects of Se[58] and its bioavailability for agriculture.[4] With changing rain patterns and increased biomass burning in the US,[59] there is also a growing need for more recent Se data, currently not possible with our pre-2011 IMPROVE dataset. Interannual variability is observed in the IMPROVE Se data (Figure S1) and can be attributed to the decrease of Se-containing anthropogenic emissions from emission control technologies and reductions in coal power generation.[8] Future measurement campaigns using online mass spectrometers and size-resolved Se in $PM_{2.5}$ measurements can help disentangle the sources and sinks of Se within $PM_{2.5}$ and the resulting redistribution of source contributions from a changing climate. There also remain open questions about the atmospheric chemistry of Se; there is very little known about what chemical form Se is emitted and removed from the atmosphere and the transport of atmospheric Se and its chemical transformations in the atmosphere, information necessary to evaluate the distribution of Se deposition in at-risk regions.

Acknowledgement

This work was funded by the University of British Columbia. Aryeh Feinberg acknowledges support from the ETH grant ETH-39 15-2 and a Swiss National Science Foundation Early Postdoc Mobility Grant (P2EZP2_195424). We thank Andrea Stenke (ETH Zurich) for assistance with processing model output.

IMPROVE is a collaborative association of state, tribal, federal agencies, and international partners. The United States Environmental Protection Agency is the primary funding source of IMPROVE, with contracting and research support from the National Park Service. The Air Quality Group at the University of California, Davis is the central analytical laboratory of IMPROVE, with ion analysis provided by Research Triangle Institute, and carbon analysis provided by Desert Research Institute. CPC Global Unified Precipitation data is provided by the NOAA/OAR/ESRL PSL, Boulder, Colorado, USA, from their website. Selenium soil concentrations were provided by the United States Geological Survey.

Figures were created using the `MATLAB m_map` package developed by Rich Pawlowicz and is available online at www.eoas.ubc.ca/ rich/map.html.

Supporting Information Available

Code for data processing and analysis of Se time series, as well as all figures in the manuscript, can be found in the following repository.

The following Supplementary Information files are available free of charge.

- Supplementary Information
- Se seasonal profile binning methods
- Se seasonal profile of each IMPROVE site

References

(1) Rayman, M. P. Selenium and human health. *The Lancet* **2012**, *379*, 1256–1268.

(2) Gorini, F.; Sabatino, L.; Pingitore, A.; Vassalle, C. Selenium: An Element of Life Essential for Thyroid Function. *Molecules* **2021**, *26*, 7084, Number: 23 Publisher: Multidisciplinary Digital Publishing Institute.

(3) Fairweather-Tait, S. J.; Bao, Y.; Broadley, M. R.; Collings, R.; Ford, D.; Hesketh, J. E.; Hurst, R. Selenium in human health and disease. *Antioxidants & Redox Signaling* **2011**, *14*, 1337–1383.

(4) Winkel, L.; Vriens, B.; Jones, G.; Schneider, L.; Pilon-Smits, E.; Bañuelos, G. Selenium cycling across soil-plant-atmosphere interfaces: A critical review. *Nutrients* **2015**, *7*, 4199–4239.

(5) Ross, H. B. An atmospheric selenium budget for the region 30° N to 90° N. *Tellus B: Chemical and Physical Meteorology* **1985**, *37*, 78–90, Publisher: Taylor & Francis _eprint: https://doi.org/10.3402/tellusb.v37i2.14999.

(6) Feinberg, A.; Stenke, A.; Peter, T.; Winkel, L. H. E. Constraining Atmospheric Selenium Emissions Using Observations, Global Modeling, and Bayesian Inference. *Environmental Science & Technology* **2020**, *54*, 7146–7155.

(7) Song, T.; Cui, G.; Su, X.; He, J.; Tong, S.; Liu, Y. The origin of soil selenium in a typical agricultural area in Hamatong River Basin, Sanjiang Plain, China. *CATENA* **2020**, *185*, 104355.

(8) Feinberg, A.; Stenke, A.; Peter, T.; Hinckley, E.-L. S.; Driscoll, C. T.; Winkel, L. H. E. Reductions in the deposition of sulfur and selenium to agricultural soils pose risk of future nutrient deficiencies. *Communications Earth & Environment* **2021**, *2*,

1–8, Bandiera_abtest: a Cc_license_type: cc_by Cg_type: Nature Research Journals Number: 1 Primary_atype: Research Publisher: Nature Publishing Group Subject_term: Atmospheric chemistry;Element cycles;Environmental impact Subject_term_id: atmospheric-chemistry;element-cycles;environmental-impact.

(9) Haygarth, P. M.; Cooke, A. I.; Jones, K. C.; Harrison, A. F.; Johnston, A. E. Long-term change in the biogeochemical cycling of atmospheric selenium: Deposition to plants and soil. *Journal of Geophysical Research: Atmospheres* **1993**, *98*, 16769–16776, _eprint: https://onlinelibrary.wiley.com/doi/pdf/10.1029/93JD01023.

(10) Randerson, J. T.; Thompson, M. V.; Conway, T. J.; Fung, I. Y.; Field, C. B. The contribution of terrestrial sources and sinks to trends in the seasonal cycle of atmospheric carbon dioxide. *Global Biogeochemical Cycles* **1997**, *11*, 535–560, _eprint: https://onlinelibrary.wiley.com/doi/pdf/10.1029/97GB02268.

(11) Jiskra, M.; Sonke, J. E.; Obrist, D.; Bieser, J.; Ebinghaus, R.; Myhre, C. L.; Pfaffhuber, K. A.; Wängberg, I.; Kyllönen, K.; Worthy, D.; Martin, L. G.; Labuschagne, C.; Mkololo, T.; Ramonet, M.; Magand, O.; Dommergue, A. A vegetation control on seasonal variations in global atmospheric mercury concentrations. *Nature Geoscience* **2018**, *11*, 244–250, Number: 4 Publisher: Nature Publishing Group.

(12) Quinn, P. K.; Shaw, G.; Andrews, E.; Dutton, E. G.; Ruoho-Airola, T.; Gong, S. L. Arctic haze: current trends and knowledge gaps. *Tellus B: Chemical and Physical Meteorology* **2007**, *59*, 99–114, Publisher: Taylor & Francis _eprint: https://doi.org/10.1111/j.1600-0889.2006.00236.x.

(13) Roulier, M.; Bueno, M.; Coppin, F.; Nicolas, M.; Thiry, Y.; Rigal, F.; Le Hécho, I.; Pannier, F. Atmospheric iodine, selenium and caesium depositions in France: I. Spatial and seasonal variations. *Chemosphere* **2021**, *273*, 128971.

(14) Weller, R.; Wöltjen, J.; Piel, C.; Resenberg, R.; Wagenbach, D.; König-Langlo, G.;

Kriews, M. Seasonal variability of crustal and marine trace elements in the aerosol at Neumayer station, Antarctica. *Tellus B: Chemical and Physical Meteorology* **2008**, *60*, 742–752, Publisher: Taylor & Francis _eprint: https://doi.org/10.1111/j.1600-0889.2008.00372.x.

(15) Shaw, G. E. Chemical air mass systems in Alaska. *Atmospheric Environment (1967)* **1988**, *22*, 2239–2248.

(16) Eldred, R. A. Comparison of Selenium and Sulfur at Remote Sites. *Journal of the Air & Waste Management Association* **1997**, *47*, 204–211, Publisher: Taylor & Francis _eprint: https://doi.org/10.1080/10473289.1997.10464423.

(17) Hanjie, W.; Carignan, J. Reviews on atmospheric selenium: Emissions, speciation and fate. *Atmospheric Environment* **2007**, *41*, 7151–7165.

(18) Mosher, B. W.; Duce, R. A. A global atmospheric selenium budget. *Journal of Geophysical Research: Atmospheres* **1987**, *92*, 13289–13298, _eprint: https://agupubs.onlinelibrary.wiley.com/doi/pdf/10.1029/JD092iD11p13289.

(19) Amouroux, D.; Liss, P. S.; Tessier, E.; Hamren-Larsson, M.; Donard, O. F. X. Role of oceans as biogenic sources of selenium. *Earth and Planetary Science Letters* **2001**, *189*, 277–283.

(20) Blazina, T.; Winkel, L.; Läderach, A.; Wernli, H.; Kirchner, J. Examining continental and marine sources of selenium in rainfall. 2016; pp 7–8.

(21) IMPROVEProgram. `https://vista.cira.colostate.edu/Improve/improve-program/`.

(22) Malm, W. C.; Sisler, J. F.; Huffman, D.; Eldred, R. A.; Cahill, T. A. Spatial and seasonal trends in particle concentration and optical extinction in the United States. *Journal of Geophysical Research* **1994**, *99*, 1347.

(23) Feinberg, A.; Maliki, M.; Stenke, A.; Sudret, B.; Peter, T.; Winkel, L. H. E. Mapping the drivers of uncertainty in atmospheric selenium deposition with global sensitivity analysis. *Atmospheric Chemistry and Physics* **2020**, *20*, 1363–1390, Publisher: Copernicus GmbH.

(24) Hyslop, N. P.; Trzepla, K.; White, W. H. Assessing the Suitability of Historical PM2.5 Element Measurements for Trend Analysis. *Environmental Science & Technology* **2015**, *49*, 9247–9255, Publisher: American Chemical Society.

(25) NCEP North American Regional Reanalysis (NARR): NOAA Physical Sciences Laboratory. `https://psl.noaa.gov/data/gridded/data.narr.pressure.html#source`.

(26) Fioletov, V. E.; McLinden, C. A.; Krotkov, N.; Li, C.; Joiner, J.; Theys, N.; Carn, S.; Moran, M. D. A global catalogue of large SO<sub>2</sub> sources and emissions derived from theOzone Monitoring Instrument. *Atmospheric Chemistry and Physics* **2016**, *16*, 11497–11519.

(27) Floor, G. H.; Román-Ross, G. Selenium in volcanic environments: A review. *Applied Geochemistry* **2012**, *27*, 517–531.

(28) Hoesly, R. M.; Smith, S. J.; Feng, L.; Klimont, Z.; Janssens-Maenhout, G.; Pitkanen, T.; Seibert, J. J.; Vu, L.; Andres, R. J.; Bolt, R. M.; Bond, T. C.; Dawidowski, L.; Kholod, N.; Kurokawa, J.-i.; Li, M.; Liu, L.; Lu, Z.; Moura, M. C. P.; O'Rourke, P. R.; Zhang, Q. Historical (1750–2014) anthropogenic emissions of reactive gases and aerosols from the Community Emissions Data System (CEDS). *Geoscientific Model Development* **2018**, *11*, 369–408, Publisher: Copernicus GmbH.

(29) Lana, A.; Bell, T. G.; Simó, R.; Vallina, S. M.; Ballabrera-Poy, J.; Kettle, A. J.; Dachs, J.; Bopp, L.; Saltzman, E. S.; Stefels, J.; Johnson, J. E.; Liss, P. S. An updated climatology of surface dimethlysulfide concentrations and

emission fluxes in the global ocean. *Global Biogeochemical Cycles* **2011**, *25*, _eprint: https://onlinelibrary.wiley.com/doi/pdf/10.1029/2010GB003850.

(30) Nightingale, P. D.; Malin, G.; Law, C. S.; Watson, A. J.; Liss, P. S.; Liddicoat, M. I.; Boutin, J.; Upstill-Goddard, R. C. In situ evaluation of air-sea gas exchange parameterizations using novel conservative and volatile tracers. *Global Biogeochemical Cycles* **2000**, *14*, 373–387, _eprint: https://onlinelibrary.wiley.com/doi/pdf/10.1029/1999GB900091.

(31) A time-averaged inventory of subaerial volcanic sulfur emissions. *Journal of Geophysical Research: Atmospheres* **1998**, *103*, 25251–25261, _eprint: https://onlinelibrary.wiley.com/doi/pdf/10.1029/98JD02091.

(32) Dentener, F.; Kinne, S.; Bond, T.; Boucher, O.; Cofala, J.; Generoso, S.; Ginoux, P.; Gong, S.; Hoelzemann, J. J.; Ito, A.; Marelli, L.; Penner, J. E.; Putaud, J.-P.; Textor, C.; Schulz, M.; van der Werf, G. R.; Wilson, J. Emissions of primary aerosol and precursor gases in the years 2000 and 1750 prescribed data-sets for AeroCom. *Atmospheric Chemistry and Physics* **2006**, *6*, 4321–4344, Publisher: Copernicus GmbH.

(33) Sindelarova, K.; Granier, C.; Bouarar, I.; Guenther, A.; Tilmes, S.; Stavrakou, T.; Müller, J.-F.; Kuhn, U.; Stefani, P.; Knorr, W. Global data set of biogenic VOC emissions calculated by the MEGAN model over the last 30 years. *Atmospheric Chemistry and Physics* **2014**, *14*, 9317–9341, Publisher: Copernicus GmbH.

(34) Kim, E.; Hopke, P. K.; Paatero, P.; Edgerton, E. S. Incorporation of parametric factors into multilinear receptor model studies of Atlanta aerosol. *Atmospheric Environment* **2003**, *37*, 5009–5021.

(35) Qureshi, S.; Dutkiewicz, V. A.; Khan, A. R.; Swami, K.; Yang, K. X.; Husain, L.; Schwab, J. J.; Demerjian, K. L. Elemental composition of PM2.5 aerosols in Queens,

New York: Solubility and temporal trends. *Atmospheric Environment* **2006**, *40*, 238–251.

(36) Yudovich, Y. E.; Ketris, M. P. Selenium in coal: A review. *International Journal of Coal Geology* **2006**, *67*, 112–126.

(37) Wen, H.; Carignan, J. Reviews on atmospheric selenium: Emissions, speciation and fate. *Atmospheric Environment* **2007**, *41*, 7151–7165.

(38) Andren, A. W.; Klein, D. H.; Talmi, Y. Selenium in coal-fired steam plant emissions. *Environmental Science & Technology* **1975**, *9*, 856–858, Publisher: American Chemical Society.

(39) Ondov, J. M.; Choquette, C. E.; Zoller, W. H.; Gordon, G. E.; Biermann, A. H.; Heft, R. E. Atmospheric behavior of trace elements on particles emitted from a coal-fired power plant. *Atmospheric Environment (1967)* **1989**, *23*, 2193–2204.

(40) Tuncel, S. G.; Olmez, I.; Parrington, J. R.; Gordon, G. E.; Stevens, R. K. Composition of fine particle regional sulfate component in Shenandoah Valley. *Environmental Science & Technology* **1985**, *19*, 529–537, Publisher: American Chemical Society.

(41) Pan, Y. P.; Wang, Y. S. Atmospheric wet and dry deposition of trace elements at 10 sites in Northern China. *Atmospheric Chemistry and Physics* **2015**, *15*, 951–972, Publisher: Copernicus GmbH.

(42) Seinfeld, J. Atmospheric Chemistry and Physics: From Air Pollution to Climate Change, 3rd Edition | Wiley. `https://www.wiley.com/en-us/Atmospheric+Chemistry+and+Physics%3A+From+Air+Pollution+to+Climate+Change%2C+3rd+Edition-p-9781118947401`.

(43) Querol, X.; Alastuey, A.; Moreno, T.; Viana, M.; Castillo, S.; Pey, J.; Rodríguez, S.; Artiñano, B.; Salvador, P.; Sánchez, M.; Garcia Dos Santos, S.; Herce Garraleta, M.;

Fernandez-Patier, R.; Moreno-Grau, S.; Negral, L.; Minguillón, M.; Monfort, E.; Sanz, M.; Palomo-Marín, R.; Pinilla-Gil, E.; Cuevas, E.; de la Rosa, J.; Sánchez de la Campa, A. Spatial and temporal variations in airborne particulate matter (PM10 and PM2.5) across Spain 1999–2005. *Atmospheric Environment* **2008**, *42*, 3964–3979, Fifth International Conference on Urban Air Quality.

(44) Qie, G.; Wang, Y.; Wu, C.; Mao, H.; Zhang, P.; Li, T.; Li, Y.; Talbot, R.; Hou, C.; Yue, T. Distribution and sources of particulate mercury and other trace elements in PM2.5 and PM10 atop Mount Tai, China. *Journal of Environmental Management* **2018**, *215*, 195–205.

(45) Suess, E.; Aemisegger, F.; Sonke, J. E.; Sprenger, M.; Wernli, H.; Winkel, L. H. E. Marine versus Continental Sources of Iodine and Selenium in Rainfall at Two European High-Altitude Locations. *Environmental Science & Technology* **2019**, *53*, 1905–1917, Publisher: American Chemical Society.

(46) Joung, Y. S.; Buie, C. R. Aerosol generation by raindrop impact on soil. *Nature Communications* **2015**, *6*, 6083, Bandiera_abtest: a Cg_type: Nature Research Journals Number: 1 Primary_atype: Research Publisher: Nature Publishing Group Subject_term: Atmospheric science;Colloids;Fluid dynamics;Geophysics Subject_term_id: atmospheric-science;colloids;fluid-dynamics;geophysics.

(47) Jacob, D. L.; Yellick, A. H.; Kissoon, L. T. T.; Asgary, A.; Wijeyaratne, D. N.; Saini-Eidukat, B.; Otte, M. L. Cadmium and associated metals in soils and sediments of wetlands across the Northern Plains, USA. *Environmental Pollution* **2013**, *178*, 211–219.

(48) Morris, C. E.; Soubeyrand, S.; Bigg, E. K.; Creamean, J. M.; Sands, D. C. Mapping Rainfall Feedback to Reveal the Potential Sensitivity of Precipitation to Biological Aerosols. *Bulletin of the American Meteorological Society* **2017**, *98*, 1109–1118, Pub-

lisher: American Meteorological Society Section: Bulletin of the American Meteorological Society.

(49) Gustin, M. S.; Stamenkovic, J. Effect of Watering and Soil Moisture on Mercury Emissions from Soils. *Biogeochemistry* **2005**, *76*, 215–232.

(50) Lindberg, S. E.; Zhang, H.; Gustin, M.; Vette, A.; Marsik, F.; Owens, J.; Casimir, A.; Ebinghaus, R.; Edwards, G.; Fitzgerald, C.; Kemp, J.; Kock, H. H.; London, J.; Majewski, M.; Poissant, L.; Pilote, M.; Rasmussen, P.; Schaedlich, F.; Schneeberger, D.; Sommar, J.; Turner, R.; Wallschläger, D.; Xiao, Z. Increases in mercury emissions from desert soils in response to rainfall and irrigation. *Journal of Geophysical Research: Atmospheres* **1999**, *104*, 21879–21888, _eprint: https://onlinelibrary.wiley.com/doi/pdf/10.1029/1999JD900202.

(51) Jaeglé, L.; Martin, R. V.; Chance, K.; Steinberger, L.; Kurosu, T. P.; Jacob, D. J.; Modi, A. I.; Yoboué, V.; Sigha-Nkamdjou, L.; Galy-Lacaux, C. Satellite mapping of rain-induced nitric oxide emissions from soils. *Journal of Geophysical Research: Atmospheres* **2004**, *109*, _eprint: https://onlinelibrary.wiley.com/doi/pdf/10.1029/2004JD004787.

(52) Pisarek, P.; Bueno, M.; Thiry, Y.; Legout, A.; Gallard, H.; Le Hécho, I. Influence of tree species on selenium and iodine partitioning in an experimental forest ecosystem. *Science of The Total Environment* **2021**, 151174.

(53) Hand, J. L.; Schichtel, B. A.; Pitchford, M.; Malm, W. C.; Frank, N. H. Seasonal composition of remote and urban fine particulate matter in the United States. *Journal of Geophysical Research: Atmospheres* **2012**, *117*, _eprint: https://onlinelibrary.wiley.com/doi/pdf/10.1029/2011JD017122.

(54) Hasheminassab, S.; Daher, N.; Saffari, A.; Wang, D.; Ostro, B. D.; Sioutas, C. Spatial and temporal variability of sources of ambient fine particulate matter

(PM<sub>2.5</sub>) in California. *Atmospheric Chemistry and Physics* **2014**, *14*, 12085–12097.

(55) Kim, P. S.; Jacob, D. J.; Fisher, J. A.; Travis, K.; Yu, K.; Zhu, L.; Yantosca, R. M.; Sulprizio, M. P.; Jimenez, J. L.; Campuzano-Jost, P.; Froyd, K. D.; Liao, J.; Hair, J. W.; Fenn, M. A.; Butler, C. F.; Wagner, N. L.; Gordon, T. D.; Welti, A.; Wennberg, P. O.; Crounse, J. D.; St. Clair, J. M.; Teng, A. P.; Millet, D. B.; Schwarz, J. P.; Markovic, M. Z.; Perring, A. E. Sources, seasonality, and trends of southeast US aerosol: an integrated analysis of surface, aircraft, and satellite observations with the GEOS-Chem chemical transport model. *Atmospheric Chemistry and Physics* **2015**, *15*, 10411–10433.

(56) Atkinson, R.; Aschmann, S. M.; Hasegawa, D.; Thompson-Eagle, E. T.; Frankenberger, W. T. Kinetics of the atmospherically important reactions of dimethyl selenide. *Environmental Science & Technology* **1990**, *24*, 1326–1332, Publisher: American Chemical Society.

(57) Xu, X.; Feng, X.; Lin, H.; Zhang, P.; Huang, S.; Song, Z.; Peng, Y.; Fu, T.-M.; Zhang, Y. Modelling the High Mercury Wet deposition in the Southeastern US by WRF-GC. *Geoscientific Model Development Discussions* **2022**, 1–21, Publisher: Copernicus GmbH.

(58) Ahmed, C. M. S.; Cui, Y.; Frie, A. L.; Burr, A.; Kamath, R.; Chen, J. Y.; Rahman, A.; Nordgren, T. M.; Lin, Y.-H.; Bahreini, R. Exposure to Dimethyl Selenide (DMSe)-Derived Secondary Organic Aerosol Alters Transcriptomic Profiles in Human Airway Epithelial Cells. *Environmental Science & Technology* **2019**, *53*, 14660–14669.

(59) Beyene, M. T.; Leibowitz, S. G.; Dunn, C. J.; Bladon, K. D. To burn or not to burn: An empirical assessment of the impacts of wildfires and prescribed fires on trace element concentrations in Western US streams. *Science of The Total Environment* **2023**, *863*, 160731.